Stereoselective Hydrolysis of Quaternary Quinuclidinium Benzoates Catalyzed by Butyrylcholinesterase

Ines Primožič,*[a] Tomica Hrenar,[a] Srđanka Tomić,[a] and Zlatko Meić[a]

Keywords: Enzyme catalysis / Hydrolysis / Kinetics / Molecular modeling

Four chiral, quaternary, *N*-methyl and *N*-benzyl derivatives of (*R*)- and (*S*)-quinuclidin-3-yl benzoates were synthesized and studied as substrates of horse serum butyrylcholinesterase (BChE). The k_{cat} for the substrates decreased in the order (*R*)-*N*-methyl > (*R*)-*N*-benzyl (2.3-fold slower) >> (*S*)-*N*-methyl (70.5-fold slower reaction), while for the (*S*)-*N*-benzyl ester inhibition of the enzyme was observed. The kinetics of inhibition (K_a = 3.3 μM) indicated that binding to the catalytic site of BChE occurred. From the ratio of the k_{cat}/K_M values of both enantiomers an enantiomeric excess of 95% was calculated for *N*-methyl derivatives. Thus, BChE is suitable as a biocatalyst for the resolution of racemic quaternary quinuclidinium esters. In order to explain the experimental data, combined quantum chemical (HF/3–21G*) and semiempirical (PM3) calculations within the ONIOM scheme of the stable species in the acylation step were performed. Geometry optimizations were carried out for all benzoate esters for an assumed active site model of BChE. It was confirmed that hydrolysis is affected to an appreciable extent by a proper geometrical orientation of substrates at the choline subsite. The energies of the optimized systems were in good agreement with the experimental data.

Introduction

Quinuclidine compounds display a wide variety of biological activities and several esters of quinuclidin-3-ol are even commercially available as therapeutic agents.[1] They have also been shown to be potential antidotes against poisoning by organophosphorus compounds such as pesticides, insecticides and chemical warfare agents.[2] Since quinuclidin-3-ol contains an asymmetric carbon atom, preparation of its esters leads to racemates. Racemates of pharmaceuticals are regarded with suspicion since enantiomers of a given bioactive compound can cause different biological effects, ranging from lower (although positive) activity of a less active enantiomer to no response at all or even to increased toxicity. Therefore, the resolution of quinuclidin-3-ol derivatives has been addressed using chemical[3−5] and biocatalytic[6,7] methods. One of the enzymes tested as a biocatalyst was butyrylcholinesterase from horse serum (BChE, EC 3.1.1.8). Although until now this enzyme has not been much investigated as a catalyst in organic synthesis, it was shown that it could accept as substrates compounds with diverse structures. It is known that BChE hydrolyses positively charged esters of choline (from acetyl to heptanoyl and benzoyl esters), some neutral esters (e.g. α-naphthyl acetate and *o*-nitrophenyl butyrate) and a number of ester drugs such as heroin, aspirin and succinylcholine.[8] BChE has also been used in the synthesis of peptides and lipopeptides for selective and mild removal of the choline ester used as a solubilizing, protecting and activating group at the *C*-terminal end.[9] Furthermore, BChE selectively hydrolyses cocaine enantiomers,[10] the structures of which are somewhat similar to quinuclidine esters. In the case of quinuclidines, BChE has been previously used for the resolution of racemic quinuclidin-3-yl butyrate[6] and for the hydrolysis of (*R*)- and (*S*)-quinuclidin-3-yl benzoates.[11] In both cases the stereoselectivity of the hydrolyses favoured the *R*-enantiomer.

In this paper we report the synthesis of quaternary, *N*-methyl (*R*-Met, *S*-Met) and *N*-benzyl (*R*-Bzl, *S*- Bzl) derivatives of (*R*)- and (*S*)-quinuclidin-3-yl benzoates, Figure 1. Furthermore, we used these as substrates of BChE, and measured the kinetics of BChE-catalyzed hydrolyses. In order to investigate the interactions of the esters with the enzyme, we also performed quantum chemical calculations on a model system of the active site. This was possible since it is known that BChE is a serine hydrolase with a structure closely related to that of acetylcholinesterase.[12] The specific architecture of the active site of cholinesterases has been revealed by a resolved crystal structure of AChE.[13] The active site consists of several major domains: a) an esteratic site containing the active serine as part of a catalytic triad (Ser, His, Glu), b) an acyl pocket − a hydrophobic region which accommodates the acyl group of an ester, c) a choline subsite for the recognition of the substrate's quaternary ammonium group, and d) an oxyanion hole formed by the main chain N−H dipoles interacting with the carbonyl oxygen of the substrate.

[a] University of Zagreb, Faculty of Science, Department of Chemistry,
Strossmayerov trg 14, 10000 Zagreb, Croatia
Fax: (internat.) +385-1-4819-288
E-mail: ines@chem.pmf.hr

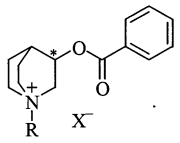

	R-Met	S-Met	R-Bzl	S-Bzl
*	R	S	R	S
R	CH_3	CH_3	$CH_2C_6H_5$	$CH_2C_6H_5$
X	I	I	Br	Br

Figure 1. Substrates for BChE

Results and Discussion

Synthesis and Enantiomeric Purity

Chiral (*R*)- and (*S*)-quinuclidin-3-ols were obtained by the resolution of racemic quinuclidin-3-yl acetates with L- and D-tartaric acid.[3] *N*-methyl- and *N*-benzyl derivatives of (*R*)- and (*S*)-quinuclidin-3-yl benzoates were synthesized by esterification of quinuclidin-3-ol with benzoic anhydride, followed by quaternization of the appropriate chiral esters with methyl iodide or benzyl bromide. The structure and purity of all compounds were determined by HPLC, IR, MS, elemental analyses, one- and two-dimensional ^1H and ^{13}C NMR spectroscopy. Optical purities were checked by optical rotation measurements and ^1H NMR spectroscopy using a chiral solvating agent. It is known that (*R*)- and (*S*)-1,1′-bi-2-naphthols are useful agents for the determination of enantiomeric purities of amino alcohols. Therefore, we investigated the potential of (*R*)-1,1′-bi-2-naphthol (RBN) as a chiral solvating agent in the case of our quaternary quinuclidinium benzoates. The spectra were recorded with a Gemini 300 MHz NMR spectrometer, using $CDCl_3$ as a solvent and adding five molar equivalents of RBN. A significant shift of quinuclidinium protons toward higher field indicated that these protons are under the influence of the ring current effect of the binaphthyl system. For the racemic *N*-methyl derivative, a splitting of the quinuclidinium 4-H resonance into two signals at $\delta = 1.97$ and 2.08 ppm was observed, the magnitude of the nonequivalence ($\Delta\Delta\delta$) being 31.8 Hz. In the case of the (±) *N*-benzyl derivative, we found two signals at $\delta = 1.78$ and 1.86 ppm ($\Delta\Delta\delta$ = 27.5 Hz). From the spectra of each enantiomer we determined that the signal at higher field belongs to the (*S*)-enantiomer. The 4-H proton resonances were assigned by the use of 2D 1H COSY spectra: NOE cross peaks of this signal with the quinuclidinium 3-H, 5-H, and 7-H protons were observed.

Hydrolyses Kinetics

BChE hydrolysis involves an active serine residue, and the overall catalytic process proceeds in a three-step mechanism: initial formation of an enzyme-substrate complex, an acylation step, and deacylation by hydrolysis,[14] Scheme 1. In the reaction sequence, E, S, ES, and EA represent free enzyme, substrate, Michaelis complex, and acylenzyme intermediate, respectively. P^1 (alcohol) and P^2 (acid) are products of the hydrolysis.

$$E + S \underset{k_{-1}}{\overset{k_1}{\rightleftharpoons}} ES \xrightarrow{k_2} EA + P^1 \xrightarrow[H_2O]{k_3} E + P^2$$

Scheme 1

Analyses of the hydrolysis kinetics of all compounds revealed that *R*-Met, *S*-Met and *R*-Bzl are substrates of BChE while for *S*-Bzl, no hydrolyses was observed under experimental conditions. The obtained kinetic constants and standard errors for substrates are displayed in Table 1.

Table 1. Michaelis−Menten parameters for BChE-catalyzed hydrolysis

Substrate	K_M/ mM [a]	k_{cat}/ min^{-1} [b]	(k_{cat}/K_M)/ 10^7 M^{-1} min^{-1} [c]
R-Met	0.127 ± 0.003	13600 ± 130	10.7
S-Met	0.065 ± 0.007	193 ± 7	0.3
R-Bzl	0.023 ± 0.004	5800 ± 270	25.2

[a] K_M corresponds to $(k_{-1}/k_1 + k_2/k_1)[k_3/(k_2 + k_3)]$. [b] k_{cat} is equal to $k_2k_3/(k_2 + k_3)$. [c] (k_{cat}/K_M) is equal to $k_1k_2/(k_{-1} + k_2)$.

The k_{cat} value for the substrates decreases in the order *R*-Met > *R*-Bzl (2.3-fold slower) >> *S*-Met (70.5-fold slower reaction). This is in agreement with previous observations that the (*R*)-enantiomer of quinuclidin-3-yl benzoate is the more active stereoisomer. On the other hand, the acylation rate constant, k_{cat}/K_M, decreases in the order *R*-Bzl > *R*-Met >> *S*-Met. Therefore, the highest substrate specificity of BChE is for *R*-Bzl. The *S*-Bzl ester acts as a reversible inhibitor of the enzyme. The enzyme-inhibitor dissociation constant K_a was calculated from the equation $K_{app} = K_a + (K_a/K_M)\cdot s$, where K_{app} is the apparent enzyme-inhibitor dissociation constant at a given substrate concentration (s) and K_M is the Michaelis constant for the substrate. The enzyme-inhibitor dissociation constant obtained was 3.3 ± 0.2 μM. The kinetics of inhibition by *S*-Bzl indicated that this compound was bound to the catalytic site of BChE. Because of the relatively small k_2, K_M can be used as a measure of the binding affinity of *S*-Met. A comparison of the K_M and K_a values shows that *S*-Bzl binds to BChE 20-fold more potently than *S*-Met.

The (*R*)-enantiomers of quaternary quinuclidinium benzoates tested are better substrates for BChE than their nonquaternized analogue, (*R*)-quinuclidin-3-yl benzoate.[11] Hydrolysis of the *R*-Met derivative is 3.1-fold faster while that of *R*-Bzl is 1.3-fold faster than the reaction of (*R*)-quinuclidin-3-yl benzoate. The hydrolysis of *S*-Met, on the other hand, is slower than that of (*S*)-quinuclidin-3-yl benzoate, while *S*-Bzl proved to be the worst enantiomer as a substrate for BChE.

The reaction of the racemic *N*-benzyl ester proceeds approximately six-times slower (calculated and tested for 0.12 mM solution of the racemate) than that of the corresponding concentration of pure *R*-Bzl because of inhibition by the (*S*)-enantiomer. Resolution of racemic *N*-benzyl derivative can therefore be achieved by hydrolysis with BChE. Furthermore, *N*-benzyl groups can be removed by catalytic hydrogenation,[15] thus regenerating tertiary chiral quinuclidin-3-ols, which can serve as precursors for the synthesis of a variety of pharmacologically interesting analogues.

A parameter commonly used to quantify kinetic resolution catalyzed by enzymes is enantiomeric ratio (E).[16] It is

a dimensionless number defined as the ratio of the "specificity constants"[17] for enantiomers, $(k_{cat}/K_M)^R/(k_{cat}/K_M)^S$. The expected optical purity (enantiomeric excess, *ee*) of the substrate and the product can be calculated for a chosen point of conversion from the obtained *E* value. A value of $E = 36$ is calculated for *N*-methyl derivatives, which corresponds to an enantiomeric excess of 95% at 1.0% conversion. BChE proved to be more selective toward quaternary than to their nonquaternary analogues ($E = 8$, *ee* of 78% at 1.0% conversion).[11]

Molecular Modeling

The origin of the catalytic power of AChE is known to be associated with electrostatic stabilization of the charged intermediate in the acylation step.[18,19] Because of the structural similarity of cholinesterases, the same is assumed for BChE.[12] Since the results of kinetic studies showed that the difference in k_{cat} of substrates lies in a slower benzoylation of BChE (hydrolysis of the benzoyl enzyme intermediate EA is the same for all substrates, Scheme 1), we assumed that the stability of the tetrahedral intermediate would reflect differences in the rates of acylation among enantiomers.

The proposed mechanism of acylation is given in Scheme 2. The Michaelis complex, ES, is formed in the first step, followed by the formation of the tetrahedral intermediate, ET. ET is then transformed into the benzoylenzyme intermediate, EA, and the appropriate quinuclidin-3-ol, ROH.

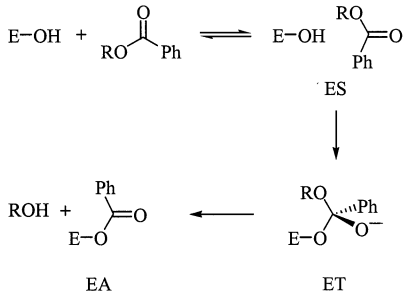

Scheme 2

The model of the active site was constructed using the 21 amino acids of the homology-built 3D model of human BChE.[13] In order to model ET, we have chosen a hybrid approach, combining quantum chemical (Hartree−Fock) and semiempirical (PM3) calculations within the ONIOM scheme. In this method, a large system is divided into two parts. One, treated quantum mechanically, was the substrate and the γ-oxygen of catalytic Ser200, while the other, bigger, part is modeled using the semiempirical method. The size of our model necessitated that the computationally intensive ab initio calculations be carried out at the HF/3−21G* level of theory. Since experimentally observed differences among enantiomers were large enough, we expected that the quantum mechanical calculations would reveal the reasons for the different behavior.

However, the relative energies obtained for ET showed that (*S*)-enantiomers, even in the case of the inhibitor *S*-Bzl, have a lower energy than that of (*R*)-enantiomers, Figure 2. Therefore, we decided to perform calculations on the Michaelis complexes (ES) and benzoylenzyme intermediates (EA) to determine the structures and relative energies of other stable species in the acylation step. In all calculations the structure of the fully optimized active site model remained close to the initial geometry. ES complexes of (*R*)-enantiomers were used as zero points of energy, Figure 2.

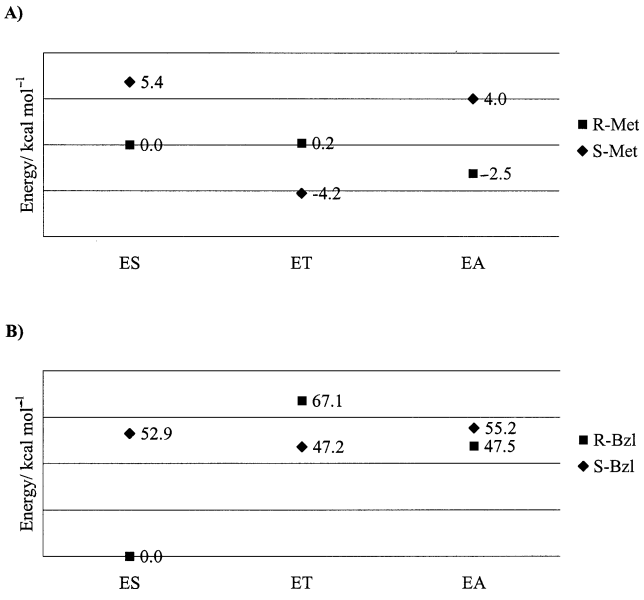

Figure 2. ONIOM (HF/PM3) calculated values of relative energies of the stable species in the acylation step of BChE-catalyzed hydrolysis: relative energies of Michaelis complexes (ES), tetrahedral intermediates (ET) and benzoylenzyme intermediates (EA) of A) *N*-methyl derivatives and B) *N*-benzyl derivatives; ES complexes of (*R*)-enantiomers were used as a reference points

Overlay of the obtained geometries of ES, ET, and EA showed that interactions with amino acids of the esteratic site, acyl pocket, and oxy anion hole are pretty much the same for all compounds. Hydrogen bond lengths involved in our model are listed in Table 2 together with other selected interatomic distances. As expected, in ES complexes we found two hydrogen bonds between the elements of the catalytic triad: one between the hydroxyl group of Ser200 and the nitrogen atom of the His440 imidazole ring and the second between the His440 imidazole amino group and the oxygen atom of Glu327. We found a third H bond, present only in ES complexes of (*S*)-enantiomers, between the carbonyl oxygen of the substrate and the amide nitrogen of Gly119.

In ET complexes we observed a complete proton transfer from Ser200 to His440 and also the elongation of the His440 N−H bond toward Glu327. ET complexes are further characterized by two hydrogen bonds between the carbonyl oxygen of the substrate and two components of the oxyanion hole (Gly118 and Gly119). Although we expected that the negative charge of the anionic tetrahedral intermediates would be stabilized by three H bonds in the oxyanion

Table 2. Selected interatomic distances for Michaelis complexes (ES), tetrahedral intermediates (ET) and benzoylenzyme intermediates (EA) for all compounds

Substrate	Complex	Distances/ Å[a] R1	R2	R3	R4	R5	R6	R7	R8	R9
	ES	0.97	1.83	1.03	1.72	3.27	4.48	3.48	3.56	3.03
R-Met	ET	1.79	1.02	1.05	1.68	1.49	3.53	2.62	2.75	3.66
	EA	5.58	4.45	1.03	1.66	1.36	4.43	3.43	3.71	3.65
	ES	0.97	1.83	1.05	1.80	3.17	4.25	3.46	2.87	3.07
S-Met	ET	1.79	1.02	1.07	1.77	1.49	3.62	2.65	2.73	3.13
	EA	5.58	5.27	1.04	1.66	1.38	4.64	3.76	3.91	5.83
	ES	0.97	1.85	1.03	1.73	3.27	4.34	3.93	3.43	4.96
R-Bzl	ET	1.78	1.01	1.05	1.68	1.43	2.80	2.61	2.69	5.03
	EA	4.41	5.54	1.03	1.76	1.37	4.37	3.43	3.66	5.80
	ES	0.97	1.81	1.03	1.71	3.11	4.02	3.52	2.79	4.14
S-Bzl	ET	1.81	1.02	1.05	1.68	1.50	3.77	2.65	2.76	4.50
	EA	3.76	3.49	1.03	1.68	1.37	4.22	3.23	3.35	5.97

[a] Distance definitions: R1−O_γ-H (Ser200); R2−$N_{\varepsilon 2}$(His440)-H_γ (Ser200); R3−$N_{\delta 1}$-$H_{\delta 1}$(His440); R4−$O_{\varepsilon 1}$(Glu327)-$H_{\delta 1}$(His440); R5−$C_{carbonyl}$(substrate)-O_γ(Ser200); R6−$O_{carbonyl}$(substrate)-N(Ala201); R7−$O_{carbonyl}$(substrate)-N(Gly118); R8−$O_{carbonyl}$(substrate)-N(Gly119); R9−N^+(substrate)-$O_{\varepsilon 1}$(Glu199).

hole,[20] that was the case only for *R*-Bzl. The missing H bond with Ala201 might be due to the fixed positions of three nitrogen atoms representing the peptide nitrogen atoms of Gly118, Gly119 and Ala201. The phenyl ring of the benzoate moieties is differently stabilized in the acyl pocket in the noncovalent adduct (ES) than in the covalent ones (ET and EA). In the ES complexes, we observed a π-π interaction between the phenyl ring and Phe331, while in the ET and EA intermediates there were also π-π interactions with Phe400 and Trp233. An analysis of the orientations of quinuclidinium moieties revealed that the chirality of quinuclidine caused the different interactions of quaternary ammonium groups at the choline subsite. The choline subsite is modelled by the side chains of Trp84, Glu199, Tyr130, and Tyr334, among which Trp84 is considered as the dominant contributor to the molecular recognition of the quaternary ammonium group of substrates, mainly via stabilizing cation−π interactions.[18,21]

Analysis of the ES complexes obtained from *N*-methyl derivatives showed that the methyl and three methylenic groups around the quaternary quinuclidinium nitrogen atom of *R*-Met have closer contacts with Trp84 and Tyr130 than those of *S*-Met, Figure 3. Both enantiomers have similar interactions with the Glu199 carboxyl group, Table 2. A comparison of the geometries found for substrates in ES and ET complexes revealed that the changes in bond lengths and angles upon reaction of *S*-Met result in a conformer with an increased distance between the quinuclidinium moiety and the benzoyl ring on going from ES to ET. The opposite occurred with *R*-Met, Figure 3. In the case of *R*-Met, this conformational change is accompanied by a decrease in the stabilizing interaction within the choline subsite, mainly with Glu199, while the interactions of *S*-Met remained almost the same, Table 2. Thus, the higher calculated energy of the *R*-Met ET complex relative to the *S*-Met ET complex can be attributed to the lower electrostatic stabilization of the quinuclidinium moiety in the choline subsite. On the other hand, in *R*-Met ES and EA complexes there are stronger interactions with the components of the choline subsite compared to those of appropriate *S*-Met complexes, and lower energies were obtained (Figure 2 and 3).

Although there is a considerable increase in the distances from the *N*-benzyl quinuclidinium moieties to the Glu199 carboxyl group compared with those from *N*-methyl quinuclidinium rings, the lower value of the calculated energy of the *S*-Bzl ET complex compared to *R*-Bzl can be explained in the same manner as for the *N*-methyl derivatives, Table 2. However, the difference in energies of ES complexes is not only affected by different interactions in the choline subsite but also by the steric requirements of accommodating a relatively large benzyl group. The *N*-benzyl group of *R*-Bzl is oriented toward Asp72 (the rim of the catalytic site gorge) while the same group of *S*-Bzl is oriented toward Tyr334 and surrounded by Trp84, Ala330, and Trp432. Considerable reorientations of Trp84 from its initial position were only noticed in complexes of *S*-Bzl, Figure 4. Steric repulsions with the benzyl group are balanced by that repositioning.

Furthermore, the configuration of the active site demands that the productive binding of *S*-Bzl (ES complex) results in an unfavourable conformation of high energy. That conformation is destabilized by the repulsion of two hydrogen atoms (quinuclidinium 7-H and benzoyl 2-H) that lie within each other's van der Waals radius (1.99 Å), Figure 5. Furthermore, the nearest atoms of two aromatic rings are at a distance of 2.90 Å. A much more relaxed conformer is obtained for ET, which is indicated by the aromatic rings' distance (5.20 Å) but there is still another direct interaction (2.06 Å) between the benzoyl (2-H) and quinuclidinium (8-H) hydrogen atoms.

Therefore, in the case of the *N*-methyl derivatives, less favourable interactions in the choline subsite of *S*-Met ES complex dictate the slower rate of hydrolysis. On the other hand, steric occlusion represents a primary determinant of substrate selectivity and enantiomeric preference of BChE

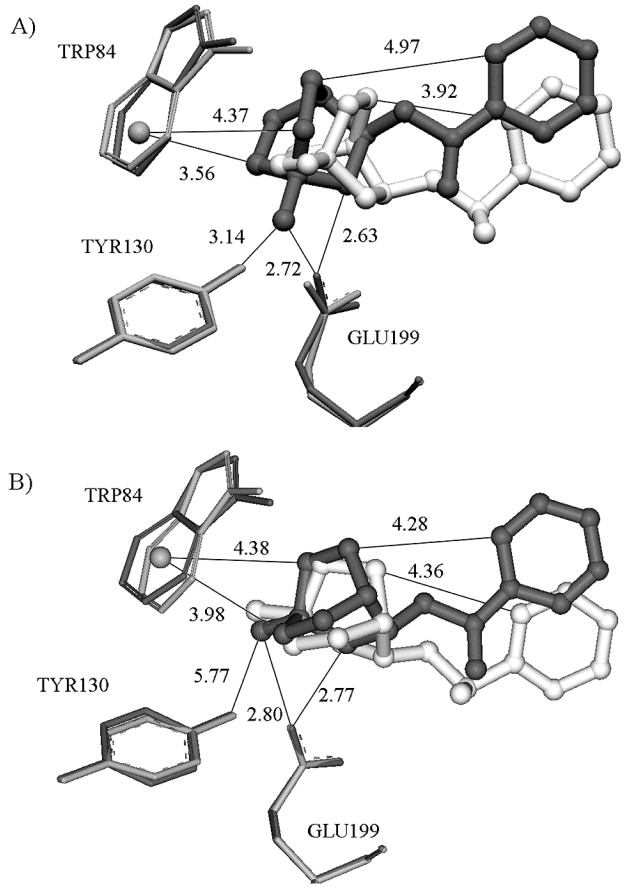

Figure 3. Comparison of the calculated structures of substrate in ES (grey) and ET (white) complexes of A) R-Met and B) S-Met within the choline subsite represented by three structurally important amino acids; hydrogen atoms are omitted for clarity; interatomic distances between atoms of the substrates in ES complexes and oxygen atoms of Glu199, Tyr130 and the centre of the benzene ring of Trp84 as well as intramolecular distances are given in Å

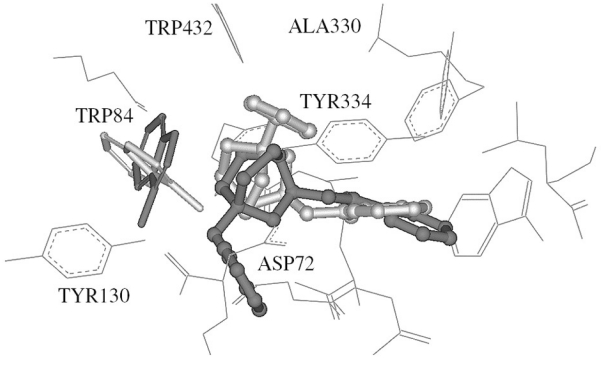

Figure 4. Structures of substrate in ES complexes of *R*-Bzl (grey) and *S*-Bzl (white) are superimposed, showing the interaction of the benzyl group in the choline subsite: hydrogen atoms are omitted for clarity; positions of amino acids are as calculated for the ES complex of *R*-Bzl; only the position of Trp84 in both complexes is shown

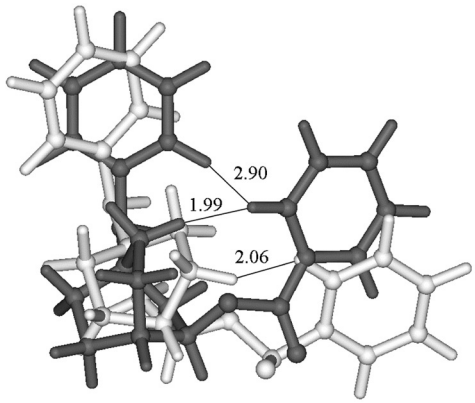

Figure 5. Structures of the substrate in a Michaelis complex (ES, grey) and a tetrahedral intermediate (ET, white) of *S*-Bzl are superimposed; interatomic distances are given in Å

toward the *N*-benzyl derivatives. For (*S*)-enantiomers, alternative binding modes in the active gorge obviously compete with those which lead (*S*-Met) or can lead (*S*-Bzl) to the tetrahedral intermediate and hydrolysis.

Conclusion

We have prepared enantiomerically pure benzoate esters of chiral quaternary *N*-methyl- and *N*-benzylquinuclidin-3-ol and found that (*R*)-1,1′-bi-2-naphthol could be used as a chiral shift reagent in ^{1}H NMR spectroscopy for determination of the optical purity of these compounds.

The kinetics of hydrolysis of chiral esters catalyzed by BChE revealed that hydrolysis proceeds in a stereoselective manner. Thus the (*R*)-enantiomers were hydrolyzed preferentially, indicating that BChE can be used as a biocatalyst in preparations of optically pure tertiary and quaternary quinuclidin-3-ols.

Despite the limitations of our model, such as a relatively small basis set, complete neglect of electron correlation within the HF method, and a small model of the protein active site, the results explain, to a reasonable degree, differences between the kinetics of the enantiomers tested. We have shown that the substrate selectivity and enantiomeric preference of BChE, as well as rates of hydrolysis, are all governed in large part by the electrostatic interactions and steric limitations of the choline subsite. Optimal positioning of the *S*-Bzl in the active site resulted in obvious steric hindrance, explaining why this enantiomer is a poor substrate for the enzyme.

Experimental Section

General Remarks: Melting points were determined in open capillaries using a Büchi B-540 melting point apparatus and are uncorrec-

ted. Specific optical rotation values were determined with an Optical Activity LTD automatic polarimeter AA-10 on 589 nm at ambient temperature (approx. 24 °C) in methanol. Elemental analyses were performed with a Perkin−Elmer PE 2400 Series II CHNS/O Analyser. IR spectra were recorded with a Perkin−Elmer FTIR 1725 X spectrometer. ^{1}H and ^{13}C 1D and 2D NMR spectra were recorded with a Varian XL-GEM 300 spectrometer at room temperature. Chemical shifts are given in ppm downfield from TMS as internal standard. ^{1}H NMR experiments with chiral shift reagent were done by dissolving 25 μmol of compound and 125 μmol (5 equiv.) of (*R*)-1,1′-bi-2-naphthol (RBN, Aldrich Chem. Co.) in 1 mL of $CDCl_3$. Only the quinuclidinium proton resonances are presented. HPLC analyses (Thermo Separation Products, SpectraSYSTEM 2000) were performed on an RP18 (Waters, SymmetryShield, 5 μm, 3.9×150 mm) column (40 °C). The mobile phase used was water/methanol/acetonitrile/acetic acid/triethylamine (60:25:15:0.33:0.2), flow rate 0.7 mL/min (*R*- and *S*-Met) and 1 mL/min (*R*- and *S*-Bzl). The reactions were carried out in a Heidolph UNIMAX 1100 Shaker.

BChE (EC, 3.1.1.8), type IV-S lyophilized powder from horse serum (Sigma Chemical Co.) was used without further purification. The hydrolysis of benzoate esters catalyzed by BChE was monitored by following the production of benzoic acid by HPLC analysis as described previously.[11] Hydrolyses were measured over a range of substrate concentrations between $0.3 \cdot K_M$ and $3 \cdot K_M$, except for *R*-Bzl (0.025−0.140 mM). All experiments for (*R*)-enantiomers were performed with 1.5×10^{-9} M and for (*S*)-enantiomers with 1.5×10^{-8} M concentration of BChE. K_M and k_{cat} values were obtained by nonlinear regression of experimental data to the Michaelis−Menten equation. The dissociation constant of enzyme-inhibitor complex for *S*-Bzl was determined from a Hunter−Downs plot, using 0.01 mM and 0.02 mM concentrations of inhibitor and *R*-Bzl as a substrate.

General Procedure: (*R*)- and (*S*) quinuclidin-3-yl benzoates were prepared according to the published procedure.[11] *N*-quaternary derivatives were prepared by the addition of methyl iodide (4 equivalents) or benzyl bromide (2 equivalents) to a solution of the appropriate chiral quinuclidin-3-yl benzoate in dry diethyl ether.

(*R*)-3-Benzoyloxy-1-methylquinuclidinium Iodide (*R*-Met): Recrystallization from methanol/diethyl ether gave white crystals, yield 320 mg (96%); m.p. 177−178 °C. $[\alpha]_D = -30$ (*c* = 1, MeOH). IR (KBr): $\tilde{\nu}$ = 3058, 2955, 2874, 1717, 1600, 1584, 1487, 1275, 1115, 717 cm^{-1}. ^{1}H NMR ($CDCl_3$): δ = 1.96−2.40 (m, 4 H, 5-H, 8-H), 2.60−2.64 (m, 1 H, 4-H), 3.39 (s, 3 H, N^+-C*H*$_3$), 3.60−4.06 (m, 5 H, 6-H, 7-H, 2-H), 4.45−4.59 (m, 1 H, 2-H), 5.35−5.45 (m, 1 H, 3-H), 7.42−7.48 (m, 2 H, 3-H, 5-H *Bz*), 7.56−7.63 (m, 1 H, 4-H *Bz*), 8.03−8.08 (m, 2 H, 2-H, 6-H *Bz*) ppm. ^{1}H NMR ($CDCl_3$, RBN): δ = 1.45−1.80 (m, 4 H, 5-H, 8-H), 2.11−2.18 (m, 1 H, 4-H), 2.52 (s, 3 H, N^+-C*H*$_3$), 2.85−3.40 (m, 5 H, 6-H, 7-H, 2-H), 3.35−3.55 (m, 1 H, 2-H), 4.31−4.42 (m, 1 H, 3-H) ppm. ^{13}C NMR ($CDCl_3$): δ = 18.3 (C-5), 21.04 (C-8), 23.6 (C-4), 55.9 (C-6), 57.1 (C-7), 62.7 (C-2), 67.4 (C-3), 51.9 (N^+-*C*H$_3$), 128.4 (C-3, C-5 *Bz*), 128.5 (C-1 *Bz*), 129.6 (C-2, C-6 *Bz*), 133.5 (C-4 *Bz*), 165.3 (C=O). ESMS: *m*/*z* = 246.2 (100%) [M^+]. $C_{15}H_{20}INO_2$ (373.23): calcd. C 48.27, H 5.40, N 3.75; found C 48.50, H 5.36, N 3.77.

(*S*)-3-Benzoyloxy-1-methylquinuclidinium Iodide (*S*-Met): $[\alpha]_D$ = +29 (*c* = 1, MeOH). ^{1}H NMR ($CDCl_3$, RBN): δ = 1.45−1.80 (m, 4 H, 5-H, 8-H), 2.03−2.09 (m, 1 H, 4-H), 2.52 (s, 3 H, N^+-C*H*$_3$), 2.85−3.40 (m, 5 H, 6-H, 7-H, 2-H), 3.35−3.55 (m, 1 H, 2-H), 4.31−4.42 (m, 1 H, 3-H) ppm.

(*R*)-3-Benzoyloxy-1-benzylquinuclidinium Bromide (*R*-Bzl): Recrystallization from acetonitrile gave white crystals, yield 510 mg (90%); m.p. 241−242 °C (decomp.). $[\alpha]_D = -43$ (*c* = 1, MeOH). IR (KBr): $\tilde{\nu}$ = 3061, 2965, 2886, 1714, 1601, 1584, 1452, 1274, 1114, 1071, 766, 710 cm^{-1}. ^{1}H NMR ($CDCl_3$): δ = 1.95−2.30 (m, 4 H, 5-H, 8-H), 2.45−2.60 (m, 1 H, 4-H), 3.70−4.15 (m, 5 H, 6-H, 7-H, 2-H), 4.40−4.50 (m, 1 H, 2-H), 5.00−5.18 (m, 2 H, −CH_2− *Bzl*), 5.28−5.40 (m, 1 H, 3-H), 7.30−7.45 (m, 5 H, 3-H, 4-H, 5-H *Bzl*, 3-H, 5-H *Bz*), 7.55 (t, ^3J = 7.15 Hz, 1 H, 4-H *Bz*), 7.69 (d, ^3J = 7.15 Hz, 2 H, 2-H, 6-H *Bzl*), 8.00 (d, ^3J = 7.97 Hz, 2 H, 2-H, 6-H *Bz*) ppm. ^{1}H NMR ($CDCl_3$, RBN): δ = 1.12−1.73 (m, 4 H, 5-H, 8-H), 1.86−1.94 (m, 1 H, 4-H), 2.75−3.30 (m, 6 H, 6-H, 7-H, 2-H), 3.90−4.05 (m, 2 H, −CH_2− *Bzl*), 4.61−4.66 (m, 1 H, 3-H) ppm. ^{13}C NMR ($CDCl_3$): δ = 18.2 (C-5), 21.0 (C-8), 24.6 (C-4), 53.2 (C-6), 53.6 (C-7), 59.5 (C-2), 66.2 (−CH_2− *Bzl*), 67.5 (C-3), 126.5 (C-1 *Bzl*), 128.3 (C-3, C-5 *Bz*), 128.5 (C-1 *Bz*), 128.9 (C-3, C-5 *Bzl*), 129.5 (C-2, C-6 *Bz*), 130.2 (C-4 *Bzl*), 133.1 (C-2, C-6 *Bzl*), 133.4 (C-4 *Bz*), 165.2 (C=O) ppm. ESMS: *m*/*z* = 322.3 (100%) [M^+]. $C_{21}H_{24}BrNO_2$ (402.32): calcd. C 62.69, H 6.01, N 3.48; found C 62.40, H 5.93, N 3.49.

(*S*)-3-Benzoyloxy-1-benzylquinuclidinium Bromide (*S*-Bzl): $[\alpha]_D$ = +44 (*c* = 1, MeOH). ^{1}H NMR ($CDCl_3$, RBN): δ = 1.12−1.73 (m, 4 H, 5-H, 8-H), 1.78−1.86 (m, 1 H, 4-H), 2.75−3.30 (m, 6 H, 6-H, 7-H, H_2), 3.90−4.05 (m, 2 H, −CH_2− *Bzl*), 4.61−4.66 (m, 1 H, 3-H) ppm.

Molecular Modeling

The three-dimensional homology-built model of human BChE[13] previously reported was used to create the model of the active site. The following amino acids were used: Asp72, Gly80, Ser81, Trp84, Gly118, Gly119, Tyr130, Glu199, Ser200, Ala201, Trp233, Leu288, Glu327, Ala330, Phe331, Tyr334, Phe400, Trp432, Met439, His440 and Gly441. Free α-amino and α-carboxyl groups were changed into amides by addition of a formyl or amino group. Aromatic amino acids are represented only by the appropriate aromatic ring and the β-carbon atom as a methyl group except for His440. The positions of some atoms were fixed during the optimization: terminal carbon and nitrogen atoms of all amino acids, the C-1 atom of the phenyl ring, the carbon atom between C-3 and C-4 of the indole ring, nitrogen atoms of Gly118, Gly119 and Ala201, the β-carbon atom of Ser200 and the carbon atom of the Glu199 carboxyl group. To model ET intermediates, a covalent bond was created between the substrate and the γ-oxygen atom of Ser200 and the hydrogen atom from the serine hydroxyl group was transferred to the nitrogen atom of His440. EA intermediates were obtained by translation (3 Å) of the alcohol part of the substrate toward the exit of the active site.

Geometry optimizations were carried out using two-layer calculations (ONIOM)[22] with the Gaussian98 quantum chemical program.[23] The higher layer was constructed from the substrate molecule and the γ-oxygen atom of Ser200. For optimization of this layer, the HF/3−21G* method was used. The remaining part of our model was included in the lower layer and calculated at the semiempirical level using the PM3 method.

Acknowledgments

We thank Professor Israel Silman of the Weizmann Institute, Rehovot, Israel for providing coordinates of the theoretical structure of human BChE. We also thank Dr Dražen Vikić-Topić, Ruđer Bošković Institute, for NMR spectra and Dr Vesna Gabelica, PLIVA Pharmaceutical Industries, for the mass spectra. We are grateful to Mr. R. Mitrić for performing some calculations. This

work was supported by the Ministry of Science and Technology of the Republic of Croatia, Project Nos 119401 and 119410.

[1] M. D. Mashkovsky, L. N. Yakhontov, M. E. Kaminka, E. E. Mikhlina, *Progress in Drug Research* **1983**, *27*, 9−61.
[2] E. Reiner, M. Škrinjarić-Špoljar, S. Dunaj, V. Simeon-Rudolf, I. Primožič, S. Tomić, *Chem.-Biol. Interact.* **1999**, *119−120*, 173−181.
[3] B. Ringdahl, R. S. Jope, D. J. Jenden, *Biochem. Pharmacol.* **1984**, *33*, 2819−2822.
[4] L. H. Sternbach, S. Kaiser, *J. Am. Chem. Soc.* **1952**, *74*, 2215−2218.
[5] A. Kalir, E. Sali, E. Shirin, *Isr. J. Chem.* **1971**, *9*, 267−268.
[6] M. Rehavi, S. Maayani, M. Sokolovsky, *Life Sci.* **1977**, *21*, 1293−1302.
[7] D. C. Muchmore, *Enantiomeric enrichment of (R,S)-3-quinuclidinol* US 5215918, **1993**.
[8] O. Lockridge, *Pharmacol. Ther.* **1990**, *47*, 35−60.
[9] M. Schelhaas, S. Glomsda, M. Hänsler, H. -D. Jakubke, H. Waldmann, *Angew. Chem. Int. Ed. Engl.* **1996**, *35*, 106−109.
[10] H. Sun, J. El Yazal, O. Lockridge, L. M. Schopfer, S. Brimijoin, Y. -P. Pang, *J. Biol. Chem.* **2001**, *276*, 9330−9336.
[11] I. Primožič, T. Hrenar, S. Tomić, Z. Meić, *J. Phys. Org. Chem.* **2002**, *58*, 608−614.
[12] P. Taylor, Z. Radic, *Annu. Rev. Pharmacol. Toxicol.* **1994**, *34*, 281−320.
[13] M. Harel, J. L. Sussman, E. Krejci, S. Bon, P. Chanal, J. Massoulie, I. Silman, *Proc. Natl. Acad. Sci. USA* **1992**, *89*, 10827−10831.
[14] D. M. Quinn, *Chem. Rev.* **1987**, *87*, 955−979.
[15] R. J. Adamski, R. E. Hackney, S. Numajiri, L. J. Spears, E. H. Yen, *Synthesis* **1973**, 221−222.
[16] C. -S. Chen, Y. Fujimoto, G. Girdaukas, C. J. Sih, *J. Am. Chem. Soc.* **1982**, *104*, 7294−7299.
[17] A. Fersht, *Enzyme Structure and Mechanism*, W. H. Freeman and Company, New York, **1985**, p. 105.
[18] D. M. Quinn, S. R. Feaster, H. K. Nair, N. A. Baker, Z. Radic, P. Taylor, *J. Am. Chem. Soc.* **2000**, *122*, 2975−2980.
[19] M. Fuxreiter, A. Warshel, *J. Am. Chem. Soc.* **1998**, *120*, 183−194.
[20] M. Harel, D. M. Quinn, H. K. Nair, I. Silman, J. L. Sussman, *J. Am. Chem. Soc.* **1996**, *118*, 2340−2346.
[21] A. Ordentlich, D. Barak, C. Kronman, N. Ariel, Y. Segall, B. Velan, A. Schafferman, *J. Biol. Chem.* **1995**, *270*, 2082−2091.
[22] F. Maseras, K. Morokuma, *J. Comput. Chem.* **1996**, *16*, 1170−1179.
[23] M. J. Frisch, G. W. Trucks, H. B. Schlegel, G. E. Scuseria, M. A. Robb, J. R. Cheeseman, V. G. Zakrzewski, J. A. Montgomery, Jr., R. E. Stratmann, J. C. Burant, S. Dapprich, J. M. Millam, A. D. Daniels, K. N. Kudin, M. C. Strain, O. Farkas, J. Tomasi, V. Barone, M. Cossi, R. Cammi, B. Mennucci, C. Pomelli, C. Adamo, S. Clifford, J. Ochterski, G. A. Petersson, P. Y. Ayala, Q. Cui, K. Morokuma, D. K. Malick, A. D. Rabuck, K. Raghavachari, J. B. Foresman, J. Cioslowski, J. V. Ortiz, A. G. Baboul, B. B. Stefanov, G. Liu, A. Liashenko, P. Piskorz, I. Komaromi, R. Gomperts, R. L. Martin, D. J. Fox, T. Keith, M. A. Al-Laham, C. Y. Peng, A. Nanayakkara, C. Gonzalez, M. Challacombe, P. M. W. Gill, B. Johnson, W. Chen, M. W. Wong, J. L. Andres, C. Gonzalez, M. Head-Gordon, E. S. Replogle, and J. A. Pople, Gaussian 98, Revision A.7, Gaussian, Inc., Pittsburgh PA, **1998**.

Received June 22, 2002
[O02351]